

Tuning superconductivity and spin-vortex instabilities in $\text{CaKFe}_4\text{As}_4$ through in-plane antisymmetric strains

Adrian Valadkhani,¹ Belén Zúñiga Céspedes²,² Salony Mandloi²,² Mingyu Xu^{3,4},^{3,4} Juan Schmidt,^{3,4} Sergey L. Bud'ko^{3,4},^{3,4} Paul C. Canfield,^{3,4} Roser Valentí¹,¹ and Elena Gati^{2,*}

¹*Institute for Theoretical Physics, Goethe University Frankfurt, 60438 Frankfurt am Main, Germany*

²*Max Planck Institute for Chemical Physics of Solids, 01187 Dresden, Germany*

³*Ames National Laboratory, U.S. Department of Energy, Iowa State University, Ames, Iowa 50011, USA*

⁴*Department of Physics and Astronomy, Iowa State University, Ames, Iowa 50011, USA*



(Received 20 July 2023; revised 12 April 2024; accepted 29 April 2024; published 8 May 2024)

Lattice strains of appropriate symmetry have served as an excellent tool to explore the interaction of superconductivity in the iron-based superconductors with orthorhombic-nematic and stripe spin-density-wave (SSDW) order. In this Letter, we contribute to a broader understanding of the coupling of strain to superconductivity and competing normal-state orders by studying $\text{CaKFe}_4\text{As}_4$ under large, in-plane strains of B_{1g} and B_{2g} symmetry. In contrast to the majority of iron-based superconductors, pure $\text{CaKFe}_4\text{As}_4$ exhibits superconductivity with a relatively high transition temperature of $T_c \sim 35$ K in proximity of a noncollinear, tetragonal, hedgehog spin-vortex crystal (SVC) order. Through experiments and calculations, we demonstrate an anisotropic in-plane strain response of T_c and the favored SVC configuration in $\text{CaKFe}_4\text{As}_4$. This supports a scenario, in which the change in spin fluctuations dominates the strain response of superconducting T_c . Overall, by suggesting moderate B_{2g} strains as an effective parameter to change the stability of SVC and SSDW, we outline a pathway to a unified phase diagram of iron-based superconductivity.

DOI: [10.1103/PhysRevB.109.L180503](https://doi.org/10.1103/PhysRevB.109.L180503)

The phase diagrams of high-temperature superconductors typically show various competing ordering tendencies, the fluctuations of which might be considered as the main pairing glue for superconductivity [1]. It is often found that the competing electronic orders are accompanied by the formation of a pronounced in-plane anisotropy [2–4]. This observation has initiated a huge surge in using external stresses and strains of appropriate symmetry, that couple directly to the anisotropic electronic state [5–11], as a tool to explore the role of its fluctuations for superconductivity.

In this context, iron-based superconductors have served as prime examples to explore and establish the intimate connection between anisotropic electronic states and superconductivity. Many of the members of this family, such as $Ae_{1-x}A_x\text{Fe}_2\text{As}_2$ ($Ae = \text{Ba, Sr, Ca}$ and $A = \text{K, Na}$) or $\text{Ba}(\text{Fe}_{1-x}\text{T}_x)_2\text{As}_2$ ($T = \text{Co, Rh, Ni, Pd}$) [12] with 1:2:2 stoichiometry, show superconductivity in proximity of stripe-type spin-density-wave (SSDW) magnetism [13] [see Fig. 1(a)]. The SSDW order is characterized by ordering vectors $\mathbf{Q}_{\text{SSDW}} = (\pi, 0)$ or $(0, \pi)$, which gives rise to an inequivalence between the two in-plane directions of the

high-temperature tetragonal lattice. This type of magnetism therefore results, aside from broken spin-rotational symmetry, in a spontaneous B_{2g} lattice distortion, which reduces the crystallographic symmetry from C_4 to C_2 . The order with broken lattice symmetry but preserved time-reversal symmetry is commonly referred to as nematic order. It is therefore often found to be “vestigial” to the SSDW order [14,15]. In other cases, such as FeSe [16], the nematic phase is even more prominent, as it is not accompanied by the formation of long-range SSDW order at ambient pressure.

The understanding of the normal state of iron-based superconductors has been tremendously advanced by utilizing lattice strains of different symmetry [8–11]. This was, for example, crucial in establishing the electronically driven nature of nematicity [3,7,11,17]. In order to provide compelling evidence that superconductivity benefits from this unusual, anisotropic normal state, a set of experiments recently studied the direct impact of applied lattice strains on the superconducting critical temperature T_c in a series of tetragonal 122 compounds [18,19]. They found that, whereas B_{2g} strains, which break the same symmetry as the nematic order, measurably suppress T_c both under compression and tension, the application of strain in the B_{1g} channel (i.e., a strain that is oriented 45° away from the nematic axis) has resulted in a much weaker response [19]. Based on a phenomenological Landau model, the anisotropic strain response of T_c was attributed to the coupling thereof to the nematic order parameter. This has strengthened the notion that nematic fluctuations play a key role [11,20] in boosting T_c .

*elena.gati@cpfs.mpg.de

Published by the American Physical Society under the terms of the [Creative Commons Attribution 4.0 International license](https://creativecommons.org/licenses/by/4.0/). Further distribution of this work must maintain attribution to the author(s) and the published article's title, journal citation, and DOI. Open access publication funded by Max Planck Society.

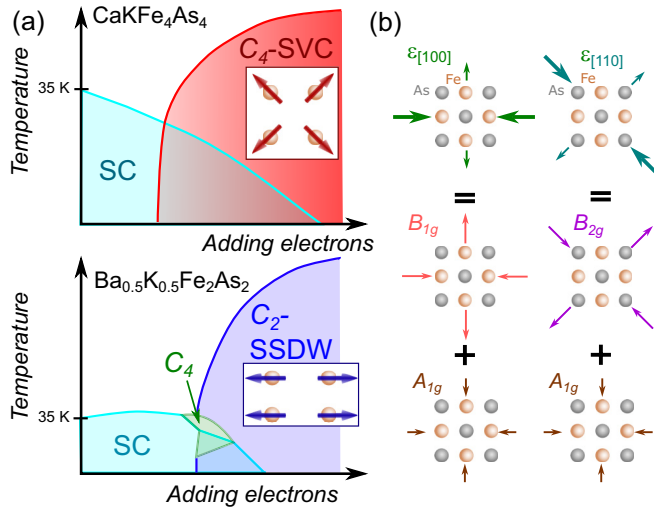


FIG. 1. (a) Schematic temperature-doping phase diagrams of the two superconductors CaKFe₄As₄ (“1144,” after Ref. [25]) and Ba_{0.5}K_{0.5}Fe₂As₂ (“122,” after Ref. [35]). Upon adding electrons to the systems, superconductivity (SC, light blue) is suppressed and magnetic phases emerge. For electron-doped 1144, the magnetic phase is the so-called spin-vortex (SVC) phase that preserves the tetragonal C₄ symmetry. In contrast, for the 122 compounds, the magnetic phase is the stripe spin-density-wave order (SSDW), which displays C₂ symmetry and is accompanied by a vestigial nematic phase. Only in proximity of both SC and C₂-SSDW order, a small region of C₄ magnetic order can be observed in the 122 compound. (b) Schematic representation of the symmetry decomposition of applied strains with respect to the tetragonal unit cell. The figure visualizes the decomposition of compressive [1 0 0] and [1 1 0] strains. The direction of applied primary stress is shown by a thick arrow. The application of stress induces a strain also perpendicular to the stress direction, the size of which is governed by the Poisson ratio. A_{1g} strains preserve the tetragonal symmetry, whereas B_{1g} and B_{2g} do not (after Ref. [8]). The induced B_{1g} and B_{2g} strains are larger than the A_{1g} strains due to the in-plane Poisson ratio (see SM [36]).

However, this notion might be questioned [21,22] by the discovery of superconductivity with very high T_c values in proximity to magnetic and charge-ordered states that preserve the tetragonal C₄ symmetry. In this context, a particular notable reference material is the quaternary compound CaKFe₄As₄, which is a superconductor with high $T_c \approx 35$ K [23,24] in its stoichiometric form, i.e., free from substitutional disorder. This superconducting state occurs in proximity of a C₄ magnetic state [25–32] [see Fig. 1(a)]. In this so-called spin-vortex-type (SVC) magnetic order—an exotic state, realized in a range of quantum materials [33]—the moments rotate clockwise/anticlockwise in an Fe plaquette [34] [$\mathbf{Q}_{\text{SVC}} = (\pi, \pi)$]. Importantly, upon tuning by doping and hydrostatic pressure [25,28,29,31], so far no C₂ symmetric order has been identified. Despite the absence of a static nematic transition, the possible presence of nematic fluctuations at ambient pressure has been discussed, but is controversial. Whereas measurements of the Young’s modulus [30] were interpreted to show signatures of nematic fluctuations, the interpretation of Raman scattering experiments suggested their absence [21]. Overall, the observations on CaKFe₄As₄

have motivated proposals that isotropic magnetic fluctuations, related to the SVC order, are sufficient to generate high-temperature superconductivity [21,22].

Clearly, CaKFe₄As₄ presents a unique and possibly much richer platform to explore the coupling of superconductivity and its normal-state properties to in-plane strains, compared to the majority of iron-based superconductors with prominent SSDW magnetism and nematicity [see Fig. 1(a)]. Yet, the evolution of the superconductivity and magnetism in CaKFe₄As₄ has not been studied under large, tunable in-plane strains, even though such studies promise key insights for developing a unified understanding of the phase diagram of iron-based superconductors.

In this Letter, we combine experiments and density-functional theory (DFT) calculations to shed light on this issue. We first demonstrate that the superconducting T_c of CaKFe₄As₄ shows a strongly anisotropic response under antisymmetric in-plane strains of B_{1g} and B_{2g} symmetry, reminiscent of the findings in 122 compounds. Whereas T_c is strongly suppressed by compressive and tensile B_{2g} strains, it is only weakly affected by B_{1g} strains. We then show through calculations, that the tendency towards the formation of magnetic order shows a strongly anisotropic response to different in-plane strains. Specifically, moderate, experimentally achievable, in-plane strains of B_{2g} symmetry offer an excellent mean to change the preference from an SVC to SSDW state. In contrast, B_{1g} strains leave the preference for SVC unchanged. The similarity of the strain response of superconductivity and magnetism motivates to attribute anisotropic strain responses not only to coupling to nematicity, but also to coupling to magnetism. With our results, we provide important insights to a broader understanding of strain tuning of the multiple phases in iron-based superconductors and beyond.

For clarity, we will use the notion of irreducible strains throughout this paper. For the tetragonal unit cell of CaKFe₄As₄, there are two antisymmetric irreducible strains, denoted by $\epsilon_{B_{1g}}$ and $\epsilon_{B_{2g}}$, which break C₄ symmetry. In this Letter, B_{1g} and B_{2g} refer to the irreducible representations of the tetragonal point group associated with the actual crystallographic unit cell rather than the one-Fe unit cell. As schematically shown in Fig. 1(b), $\epsilon_{B_{1g}}$ and $\epsilon_{B_{2g}}$ strains are primarily induced when stress is applied along the crystallographic [1 0 0] and [1 1 0] directions, respectively, in addition to a smaller fully symmetric strain $\epsilon_{A_{1g}}$. The used decomposition procedure is described in the Supplemental Material (SM) [36]. Tensile (compressive) strains are denoted throughout our work by positive (negative) signs.

We first demonstrate how the superconducting critical temperature T_c changes with these in-plane antisymmetric strains through experiments. To this end, oriented CaKFe₄As₄ crystals [37] (along [1 0 0] and [1 1 0]) were mounted on rigid platforms [38,39]. Varying strains were applied to the platform and the sample with a piezoelectric-actuator-based uniaxial pressure cell [5]. T_c was determined through temperature-dependent measurements of the mutual inductance of two concentric coils [5] wound around the platform with the sample (see SM Sec. A for details).

Figure 2 shows the temperature dependence of the mutual inductance, M , at different strains of type $\epsilon_{B_{2g}}$ [Figs. 2(a) and

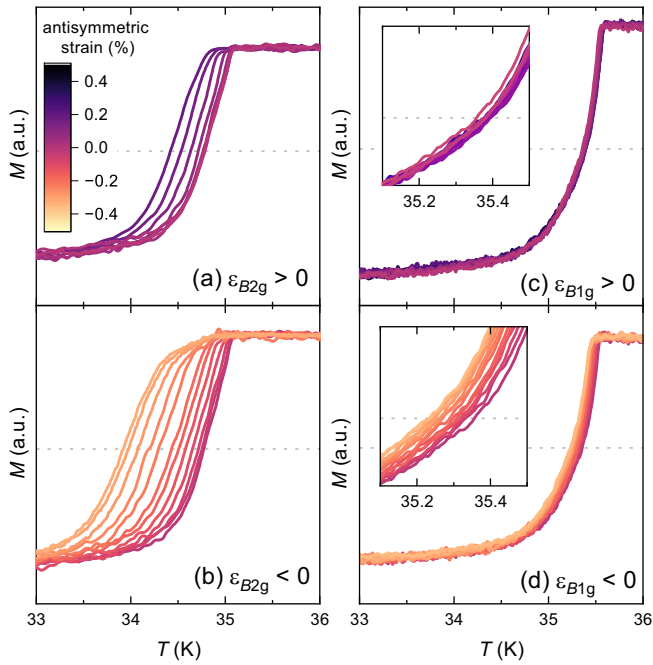


FIG. 2. Mutual inductance data on $\text{CaKFe}_4\text{As}_4$ as a function of temperature for different applied, antisymmetric strains (a), (b) $\epsilon_{B_{2g}}$ and (c), (d) $\epsilon_{B_{1g}}$. Top (bottom) panels show data under tensile (compressive) strains. The spacing in strain between two data sets amounts to $\sim 0.05\%$. The gray dashed line visualizes the 50% threshold that is used to infer T_c .

2(b)] and $\epsilon_{B_{1g}}$ [Figs. 2(c) and 2(d)]. In each figure, the top (bottom) panel shows the data taken under tensile (compressive) strains. The superconducting transition is clearly identified in all data sets by a sharp drop of M and we assign T_c to the temperature where M has reached 50% of its full value (see the gray dashed line). The bare M data reveal clearly our main experimental findings. First, the response of T_c to $\epsilon_{B_{2g}}$ is larger than the one to $\epsilon_{B_{1g}}$ strain (note the same scale of the temperature axes in all plots). Second, both compressive and tensile $\epsilon_{B_{2g}}$ strains suppress T_c . The suppression is as large as $\Delta T_c \sim -0.8$ K by $\epsilon_{B_{2g}} \sim -0.4\%$.

To further quantify the statements above, we compiled the phase diagram as $\Delta T_c = T_c(\epsilon) - T_c(\epsilon = 0)$ up to $\pm 0.4\%$ antisymmetric strains (and $\pm 0.2\%$ symmetric strains) in Fig. 3. The color shaded areas around the $T_c(\epsilon)$ data indicate the width of the superconducting transition at each ϵ , determined from 25% and 75% threshold values.

By consideration of symmetry-allowed terms in a Ginzburg-Landau approach [14,18], it is expected that, to lowest order, $\Delta T_c(\epsilon) \sim D_{A_{1g}}\epsilon_{A_{1g}} + D_i\epsilon_i^2$ with $i = B_{1g}$ or B_{2g} . The linear strain dependence can only result from the dependence of T_c on $\epsilon_{A_{1g}}$, which are also induced in our experiments.

Figure 3 shows that the data of T_c vs $\epsilon_{B_{2g}}$ is clearly dominated by the quadratic strain dependence, expected for antisymmetric strains, over almost the full strain range. A polynomial fit of order two (see the dashed line) yields the quadratic coefficient $D_{B_{2g}}/T_c(0) = -(2780 \pm 50)$. Only for high compression ($|\epsilon| \gtrsim 0.3\%$), small deviations from the quadratic behavior are observed, which, however, are still within the error bars of our experiment.

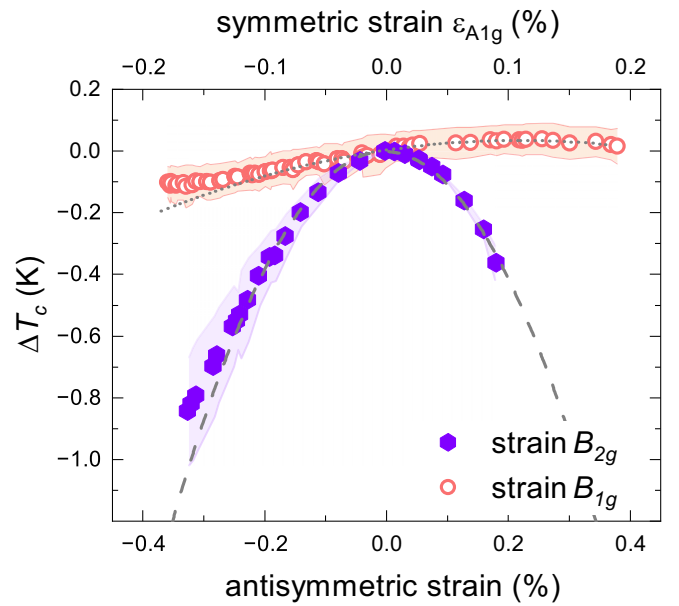


FIG. 3. Change of superconducting critical temperature of $\text{CaKFe}_4\text{As}_4$, $\Delta T_c = T_c(\epsilon) - T_c(\epsilon = 0)$ with antisymmetric $\epsilon_{B_{2g}}$ (solid symbols) and $\epsilon_{B_{1g}}$ (open symbols) strains (bottom axis). In both experiments under large B_{1g} and B_{2g} strains, a small, but finite symmetric A_{1g} strain is induced as well and depicted on the top axis. The color shading represents the width of the transition. Dashed and dotted gray lines correspond to polynomial fits up to the second order in strain.

For the B_{1g} data, a weak quadratic change of T_c with $\epsilon_{B_{1g}}$ can also be identified, even though the linear contribution to $T_c(\epsilon)$ due to A_{1g} strains dominates. The quadratic coefficient amounts to $D_{B_{1g}}/T_c(0) = -(36 \pm 1)$, which is unlikely to result from a small misalignment of the crystal (see SM [36]) and is therefore considered intrinsic to the B_{1g} channel. Similar to the B_{2g} data, only small deviations from the polynomial fit within the error bars of the experiment occur for $|\epsilon| \gtrsim 0.3\%$.

To explore possible correlations of $T_c(\epsilon)$ with the strain dependence of the normal-state fluctuations, we discuss in the following our results of DFT calculations under the same antisymmetric strain fields. In $\text{CaKFe}_4\text{As}_4$ at ambient conditions, no static magnetic order [22,40] can be found, but strong SVC fluctuations [22,41,42] exist. In previous computational studies, it has been shown that it is crucial to take spin fluctuations into account for accurate predictions of the ambient-pressure structure and structural transitions at high pressures [28,43,44]. In these works, the presence of spin fluctuations was simulated by imposing a “frozen” magnetic configuration within a reduced Stoner theory, in which the size of magnetic moments is adjusted for the values found in experiment in Ni-doped $\text{CaKFe}_4\text{As}_4$ [26]. Given that this approach has proven successful in exploring the coupling of magnetism to strain, we now calculate within DFT the energy of “frozen” SVC and SSDW orders in $\text{CaKFe}_4\text{As}_4$ under finite in-plane strains (see SM [36]) and use it as a proxy for the nature and strength of magnetic fluctuations. This approach indirectly also contains information on the coupling to other degrees of freedom [45].

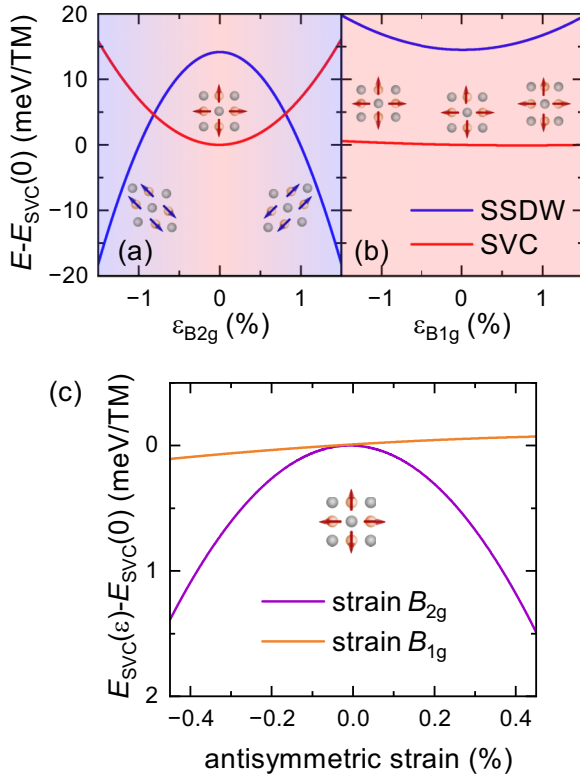


FIG. 4. (a), (b) Calculated energies of CaKFe₄As₄ for imposed “frozen” spin configurations of spin-vortex crystal (SVC) order and stripe spin-density-wave (SSDW) order as a function of antisymmetric strains of (a) B_{2g} and (b) B_{1g} symmetry. Whereas for B_{1g} strains the SVC configuration remains clearly energetically favorable, B_{2g} strains change the preferred type of spin fluctuations from SVC to SSDW around $\epsilon_{B_{2g}} \approx \pm 0.8\%$, i.e., when $E_{\text{SSDW}}(\epsilon) < E_{\text{SVC}}(\epsilon)$. The SVC (SSDW) ordering motif is visualized by red (blue) arrows in the small cartoons. (c) Enlarged view on the energy of the SVC state as a function of antisymmetric strains in the experimentally studied strain range. Note that the experimental strain range is lower than the theoretically predicted critical strain.

Consistent with earlier DFT results [28,43], the result at $\epsilon = 0$ is that a SVC configuration is energetically favored over the SSDW [$E_{\text{SVC}}(0) < E_{\text{SSDW}}(0)$]; see Fig. 4. For finite strains, the change in energy of a given magnetic configuration is, to lowest order, given by $\Delta E \sim C_{A_{1g}}\epsilon_{A_{1g}} + C_i\epsilon_i^2$ with $i = B_{1g}, B_{2g}$. The calculated energies for both SVC and SSDW magnetic configurations are well described by such a linear plus quadratic strain dependence for $\epsilon_{B_{2g}}$ [Fig. 4(a)] and $\epsilon_{B_{1g}}$ [Fig. 4(b)]. The sign and strength of the quadratic term of the strain dependence, however, strongly differ between the different orders and strains, as we discuss below.

Specifically, $\epsilon_{B_{2g}}$ strongly weakens the tendency towards the SVC configuration and promotes the one towards SSDW order [Fig. 4(a)], consistent with a symmetry analysis within a Landau approach [46], since the SSDW couples directly to $\epsilon_{B_{2g}}$ (see also Fig. 1). In contrast, the energy of the SVC configuration is only weakly increased by $\epsilon_{B_{1g}}$. At the same time, the SSDW configuration becomes significantly unfavorable under increasing $\epsilon_{B_{1g}}$ [Fig. 4(b)].

On a quantitative level, following important conclusions can be drawn. First, a B_{2g} strain of $\epsilon_{B_{2g}}^{\text{crit}} \approx \pm 0.8\%$ changes the preferred type of spin fluctuations from SVC and SSDW. We note that $\epsilon_{B_{2g}}^{\text{crit}}$ is larger than typical strains that are induced by a spontaneous nematic/SSDW distortion in the 122 pnictides ($\epsilon_{B_{2g}} \lesssim 0.3\%$) [35]. This reflects the fact that the CaKFe₄As₄ is not as close to a SSDW-nematic instability at ambient conditions as the related 122 compounds [30]. Second, for B_{1g} strains, there is hardly any change in the magnetism and the SVC configuration remains clearly favorable. Overall, this results in a clear anisotropy of the antisymmetric strain dependence of the magnetic energies of the SVC order of $(C_{B_{2g}}/C_{B_{1g}})_{\text{SVC}} \sim 52$ [Fig. 4(c)].

The qualitatively similar anisotropic strain response of the energies for the SVC configuration in Fig. 4(c) and the experimentally determined superconducting T_c in Fig. 3 under both types of antisymmetric strains, $\epsilon_{B_{1g}}$ and $\epsilon_{B_{2g}}$, is striking and is the main result of the present Letter. We find empirically that even the magnitudes of the anisotropy parameters of T_c of $D_{B_{2g}}/D_{B_{1g}} \sim 77$ and of E of $C_{B_{2g}}/C_{B_{1g}} \sim 52$ are similar. Even though the calculated energies can only serve as a rough proxy for the spin fluctuations, it is natural to assume that in a scenario of magnetically driven superconductivity [47–49], there exists a connection of E and T_c . As a consequence, in the case of CaKFe₄As₄ with SVC configuration, which does not break tetragonal symmetry, it is the fact that $\epsilon_{B_{2g}}$ strains tend to weaken SVC fluctuations [46], while $\epsilon_{B_{1g}}$ barely do, that might be at the origin of the observed in-plane strain anisotropy of T_c . Whereas the in-plane anisotropic strain suppression of T_c is a widely observed feature in iron-based superconductors [18,19,50], it is often solely attributed to the coupling to nematicity. Importantly, this conclusion is based on the assumption that spin fluctuations are strengthened upon tuning by B_{2g} strains [51], which is expected to increase T_c . In this Letter, we present an alternative and consistent scenario for the suppression of T_c by weakened spin fluctuations.

Aside from this proposal, the suppression of nematic fluctuations by antisymmetric strains would also contribute in a similar way to $T_c(\epsilon)$ in CaKFe₄As₄. Further measurements, e.g., microscopic measurements, will shed further light onto the interesting question regarding which role each of these fluctuations play in destabilizing superconductivity with strain. Our work provides the motivation for these microscopic measurements [52–60], by strengthening the notion of CaKFe₄As₄ as an excellent model system. Specifically, the suggestion that the spin fluctuations would develop a strongly anisotropic and quadratic response to strain introduces an interesting scenario, which can be tested experimentally.

At the same time, our results clearly demonstrate a route towards a unified phase diagram of iron-based superconductivity by using antisymmetric strains in the CaKFe₄As₄ family, since these strains might be used to manipulate the relative importance of SVC and SSDW magnetism [30] for superconductivity. The theoretical prediction of the strain tunability of magnetism (see Fig. 4) within an experimentally achievable strain range motivates a series of studies in the future. For example, it would be very interesting to study superconducting properties at larger B_{2g} strains, in particular at those strains, where SSDW fluctuations become dominant.

In summary, our work on the stoichiometric high- T_c superconductor $\text{CaKFe}_4\text{As}_4$ contributes to a broader understanding of how antisymmetric strains impact superconductivity and its competing states in iron-based superconductors. We provide a plausible scenario for $T_c(\epsilon)$ in terms of suppressed spin-vortex fluctuations, which challenges established notions in iron-based superconductors. Furthermore, we highlight how antisymmetric strain tuning is an effective tool to manipulate the relative stability of noncollinear and collinear orders. It is this latter aspect which establishes antisymmetric strain tuning as a powerful tuning parameter for a wide range of magnetic quantum materials, including frustrated magnets.

We thank William Meier and Andreas Kreyssig for insightful discussions on the 1144 compounds, as well as Jack

Barraclough for useful discussions on the limitations of the strain platforms. Financial support by the Max Planck Society is gratefully acknowledged. In addition, we gratefully acknowledge funding through the Deutsche Forschungsgemeinschaft (DFG, German Research Foundation) through TRR 288-422213477 (Projects A05 and B05) and the SFB 1143 (Project-ID 247310070; Project C09). Research in Dresden benefits from the environment provided by the DFG Cluster of Excellence ct.qmat (EXC 2147, Project ID 390858940). Work at the Ames National Laboratory was supported by the U.S. Department of Energy, Office of Science, Basic Energy Sciences, Materials Sciences and Engineering Division. The Ames National Laboratory is operated for the U.S. Department of Energy by Iowa State University under Contract No. DEAC02-07CH11358.

-
- [1] E. Fradkin, S. A. Kivelson, and J. M. Tranquada, *Rev. Mod. Phys.* **87**, 457 (2015).
- [2] E. Fradkin, S. A. Kivelson, M. J. Lawler, J. P. Eisenstein, and A. P. Mackenzie, *Annu. Rev. Condens. Matter Phys.* **1**, 153 (2010).
- [3] R. M. Fernandes, A. V. Chubukov, and J. Schmalian, *Nat. Phys.* **10**, 97 (2014).
- [4] V. Hinkov, D. Haug, B. Fauque, P. Bourges, Y. Sidis, A. Ivanov, C. Bernhard, C. T. Lin, and B. Keimer, *Science* **319**, 597 (2008).
- [5] C. W. Hicks, M. E. Barber, S. D. Edkins, D. O. Brodsky, and A. P. Mackenzie, *Rev. Sci. Instrum.* **85**, 065003 (2014).
- [6] H.-H. Kim, E. Lefrançois, K. Kummer, R. Fumagalli, N. B. Brookes, D. Betto, S. Nakata, M. Tortora, J. Porras, T. Loew *et al.*, *Phys. Rev. Lett.* **126**, 037002 (2021).
- [7] J.-H. Chu, H.-H. Kuo, J. G. Analytis, and I. R. Fisher, *Science* **337**, 710 (2012).
- [8] M. S. Ikeda, T. Worasaran, J. C. Palmstrom, J. A. W. Straquadine, P. Walmsley, and I. R. Fisher, *Phys. Rev. B* **98**, 245133 (2018).
- [9] R. Willa, M. Fritz, and J. Schmalian, *Phys. Rev. B* **100**, 085106 (2019).
- [10] E. Gati, L. Xiang, S. L. Bud'ko, and P. C. Canfield, *Ann. Phys.* **532**, 2000248 (2020).
- [11] A. E. Böhmer, J.-H. Chu, S. Lederer, and M. Yi, *Nat. Phys.* **18**, 1412 (2022).
- [12] P. C. Canfield and S. L. Bud'ko, *Annu. Rev. Condens. Matter Phys.* **1**, 27 (2010).
- [13] P. Dai, *Rev. Mod. Phys.* **87**, 855 (2015).
- [14] R. M. Fernandes and A. J. Millis, *Phys. Rev. Lett.* **111**, 127001 (2013).
- [15] R. M. Fernandes, P. P. Orth, and J. Schmalian, *Annu. Rev. Condens. Matter Phys.* **10**, 133 (2019).
- [16] A. E. Böhmer and A. Kreisel, *J. Phys.: Condens. Matter* **30**, 023001 (2018).
- [17] T. Worasaran, M. S. Ikeda, J. C. Palmstrom, J. A. W. Straquadine, S. A. Kivelson, and I. R. Fisher, *Science* **372**, 973 (2021).
- [18] P. Malinowski, Q. Jiang, J. J. Sanchez, J. Mutch, Z. Liu, P. Went, J. Liu, P. J. Ryan, J.-W. Kim, and J.-H. Chu, *Nat. Phys.* **16**, 1189 (2020).
- [19] Z. Liu, Y. Gu, W. Hong, T. Xie, D. Gong, X. Ma, J. Liu, C. Hu, L. Zhao, X. Zhou *et al.*, *Phys. Rev. Res.* **1**, 033154 (2019).
- [20] S. Lederer, Y. Schattner, E. Berg, and S. A. Kivelson, *Phys. Rev. Lett.* **114**, 097001 (2015).
- [21] W.-L. Zhang, W. R. Meier, T. Kong, P. C. Canfield, and G. Blumberg, *Phys. Rev. B* **98**, 140501(R) (2018).
- [22] Q.-P. Ding, W. R. Meier, J. Cui, M. Xu, A. E. Böhmer, S. L. Bud'ko, P. C. Canfield, and Y. Furukawa, *Phys. Rev. Lett.* **121**, 137204 (2018).
- [23] A. Iyo, K. Kawashima, T. Kinjo, T. Nishio, S. Ishida, H. Fujihisa, Y. Gotoh, K. Kihou, H. Eisaki, and Y. Yoshida, *J. Am. Chem. Soc.* **138**, 3410 (2016).
- [24] W. R. Meier, T. Kong, U. S. Kaluarachchi, V. Taufour, N. H. Jo, G. Drachuck, A. E. Böhmer, S. M. Saunders, A. Sapkota, A. Kreyssig *et al.*, *Phys. Rev. B* **94**, 064501 (2016).
- [25] W. R. Meier, Q.-P. Ding, A. Kreyssig, S. L. Bud'ko, A. Sapkota, K. Kothapalli, V. Borisov, R. Valentí, C. D. Batista, P. P. Orth, R. M. Fernandes *et al.*, *npj Quantum Mater.* **3**, 5 (2018).
- [26] A. Kreyssig, J. M. Wilde, A. E. Böhmer, W. Tian, W. R. Meier, B. Li, B. G. Ueland, M. Xu, S. L. Bud'ko, P. C. Canfield *et al.*, *Phys. Rev. B* **97**, 224521 (2018).
- [27] S. L. Bud'ko, V. G. Kogan, R. Prozorov, W. R. Meier, M. Xu, and P. C. Canfield, *Phys. Rev. B* **98**, 144520 (2018).
- [28] U. S. Kaluarachchi, V. Taufour, A. Sapkota, V. Borisov, T. Kong, W. R. Meier, K. Kothapalli, B. G. Ueland, A. Kreyssig, R. Valentí, R. J. McQueeney, A. I. Goldman, S. L. Budko, and P. C. Canfield, *Phys. Rev. B* **96**, 140501(R) (2017).
- [29] L. Xiang, W. R. Meier, M. Xu, U. S. Kaluarachchi, S. L. Bud'ko, and P. C. Canfield, *Phys. Rev. B* **97**, 174517 (2018).
- [30] A. E. Böhmer, F. Chen, W. R. Meier, M. Xu, G. Drachuck, M. Merz, P. W. Wiecki, S. L. Bud'ko, V. Borisov, R. Valentí *et al.*, *arXiv:2011.13207*.
- [31] M. Xu, J. Schmidt, E. Gati, L. Xiang, W. R. Meier, V. G. Kogan, S. L. Bud'ko, and P. C. Canfield, *Phys. Rev. B* **105**, 214526 (2022).
- [32] M. Xu, J. Schmidt, M. A. Tanatar, R. Prozorov, S. L. Bud'ko, and P. C. Canfield, *Phys. Rev. B* **107**, 134511 (2023).
- [33] K. Riedl, E. Gati, D. Zielke, S. Hartmann, O. M. Vyaselev, N. D. Kushch, H. O. Jeschke, M. Lang, R. Valentí, M. V. Kartsovnik *et al.*, *Phys. Rev. Lett.* **127**, 147204 (2021).

- [34] R. M. Fernandes, S. A. Kivelson, and E. Berg, *Phys. Rev. B* **93**, 014511 (2016).
- [35] A. E. Böhmer, F. Hardy, L. Wang, T. Wolf, P. Schweiss, and C. Meingast, *Nat. Commun.* **6**, 7911 (2015).
- [36] See Supplemental Material at <http://link.aps.org/supplemental/10.1103/PhysRevB.109.L180503> for an extended method description, discussion of symmetry decompositions into irreducible strains and their coupling to the order parameters, and consequences of possible misalignments, which includes Refs. [5,8,25,25,26,28,30,37–39,43,44,61–70].
- [37] W. R. Meier, T. Kong, S. L. Bud'ko, and P. C. Canfield, *Phys. Rev. Mater.* **1**, 013401 (2017).
- [38] J. Park, J. M. Bartlett, H. M. L. Noad, A. L. Stern, M. E. Barber, M. König, S. Hosoi, T. Shibauchi, A. P. Mackenzie, A. Steppke *et al.*, *Rev. Sci. Instrum.* **91**, 083902 (2020).
- [39] J. M. Bartlett, A. Steppke, S. Hosoi, H. Noad, J. Park, C. Timm, T. Shibauchi, A. P. Mackenzie, and C. W. Hicks, *Phys. Rev. X* **11**, 021038 (2021).
- [40] S. L. Bud'ko, T. Kong, W. R. Meier, X. Ma, and P. C. Canfield, *Philos. Mag.* **97**, 2689 (2017).
- [41] T. Xie, Y. Wei, D. Gong, T. Fennell, U. Stuhr, R. Kajimoto, K. Ikeuchi, S. Li, J. Hu, and H. Luo, *Phys. Rev. Lett.* **120**, 267003 (2018).
- [42] J. Cui, Q.-P. Ding, W. R. Meier, A. E. Böhmer, T. Kong, V. Borisov, Y. Lee, S. L. Bud'ko, R. Valentí, P. C. Canfield *et al.*, *Phys. Rev. B* **96**, 104512 (2017).
- [43] V. Borisov, P. C. Canfield, and R. Valentí, *Phys. Rev. B* **98**, 064104 (2018).
- [44] G. Song, V. Borisov, W. R. Meier, M. Xu, K. J. Dusoe, J. T. Sypek, R. Valentí, P. C. Canfield, and S.-W. Lee, *APL Mater.* **7**, 061104 (2019).
- [45] V. Borisov, R. M. Fernandes, and R. Valentí, *Phys. Rev. Lett.* **123**, 146402 (2019).
- [46] W. Meier, Growth, properties and magnetism of CaKFe₄As₄, Ph.D. thesis, Iowa State University, 2018, pp. 118–122.
- [47] A. Chubukov, *Annu. Rev. Condens. Matter Phys.* **3**, 57 (2012).
- [48] P. J. Hirschfeld, *C. R. Phys.* **17**, 197 (2016).
- [49] C. Liu, P. Bourges, Y. Sidis, T. Xie, G. He, F. Bourdarot, S. Danilkin, H. Ghosh, S. Ghosh, X. Ma *et al.*, *Phys. Rev. Lett.* **128**, 137003 (2022).
- [50] Z. Zhao, D. Hu, X. Fu, K. Zhou, Y. Gu, G. Tan, X. Lu, and P. Dai, [arXiv:2305.04424](https://arxiv.org/abs/2305.04424).
- [51] T. Kissikov, R. Sarkar, M. Lawson, B. T. Bush, E. I. Timmons, M. A. Tanatar, R. Prozorov, S. L. Bud'ko, P. C. Canfield, R. M. Fernandes *et al.*, *Nat. Commun.* **9**, 1058 (2018).
- [52] R. Khasanov, W. R. Meier, Y. Wu, D. Mou, S. L. Bud'ko, I. Eremin, H. Luetkens, A. Kaminski, P. C. Canfield, and A. Amato, *Phys. Rev. B* **97**, 140503(R) (2018).
- [53] D. Jost, J.-R. Scholz, U. Zwick, W. R. Meier, A. E. Böhmer, P. C. Canfield, N. Lazarević, and R. Hackl, *Phys. Rev. B* **98**, 020504(R) (2018).
- [54] F. Lochner, F. Ahn, T. Hickel, and I. Eremin, *Phys. Rev. B* **96**, 094521 (2017).
- [55] M. Bristow, W. Knafo, P. Reiss, W. Meier, P. C. Canfield, S. J. Blundell, and A. I. Coldea, *Phys. Rev. B* **101**, 134502 (2020).
- [56] D. Mou, T. Kong, W. R. Meier, F. Lochner, L.-L. Wang, Q. Lin, Y. Wu, S. L. Bud'ko, I. Eremin, D. D. Johnson *et al.*, *Phys. Rev. Lett.* **117**, 277001 (2016).
- [57] K. Cho, A. Fente, S. Teknowijoyo, M. A. Tanatar, K. R. Joshi, N. M. Nusran, T. Kong, W. R. Meier, U. Kaluarachchi, I. Guillamon, H. Suderow, S. L. Budko, P. C. Canfield, and R. Prozorov, *Phys. Rev. B* **95**, 100502(R) (2017).
- [58] S. Teknowijoyo, K. Cho, M. Kończykowski, E. I. Timmons, M. A. Tanatar, W. R. Meier, M. Xu, S. L. Bud'ko, P. C. Canfield, and R. Prozorov, *Phys. Rev. B* **97**, 140508(R) (2018).
- [59] K. Iida, M. Ishikado, Y. Nagai, H. Yoshida, A. D. Christianson, N. Murai, K. Kawashima, Y. Yoshida, H. Eisaki, and A. Iyo, *J. Phys. Soc. Jpn.* **86**, 093703 (2017).
- [60] P. K. Biswas, A. Iyo, Y. Yoshida, H. Eisaki, K. Kawashima, and A. D. Hillier, *Phys. Rev. B* **95**, 140505(R) (2017).
- [61] M. E. Barber, A. Steppke, A. P. Mackenzie, and C. W. Hicks, *Rev. Sci. Instrum.* **90**, 023904 (2019).
- [62] P. Hohenberg and W. Kohn, *Phys. Rev.* **136**, B864 (1964).
- [63] W. Kohn and L. J. Sham, *Phys. Rev.* **140**, A1133 (1965).
- [64] P. E. Blöchl, *Phys. Rev. B* **50**, 17953 (1994).
- [65] G. Kresse and D. Joubert, *Phys. Rev. B* **59**, 1758 (1999).
- [66] G. Kresse and J. Hafner, *Phys. Rev. B* **47**, 558 (1993).
- [67] G. Kresse and J. Furthmüller, *Phys. Rev. B* **54**, 11169 (1996).
- [68] G. Kresse and J. Furthmüller, *Comput. Mater. Sci.* **6**, 15 (1996).
- [69] J. P. Perdew, K. Burke, and M. Ernzerhof, *Phys. Rev. Lett.* **77**, 3865 (1996).
- [70] C. Bradley and A. Cracknell, *The Mathematical Theory of Symmetry in Solids: Representation Theory for Point Groups and Space Groups*, EBSCO Ebook Academic Collection (Oxford University Press, Oxford, UK, 2010).